Genetic deletion of mouse platelet glycoprotein Ibβ produces a Bernard-Soulier phenotype with increased α-granule size

Kazunobu Kato, Constantino Martinez, Susan Russell, Paquita Nurden, Alan Nurden, Steven Fiering, and Jerry Ware

Here we report the characterization of a mouse model of the Bernard-Soulier syndrome generated by a targeted disruption of the gene encoding the glycoprotein (GP) Ibβ subunit of the GP Ib-IX complex. Similar to a Bernard-Soulier model generated by disruption of the mouse GP Ibα subunit, GP Ibβ^{Null} mice display macrothrombocytopenia and a severe bleeding phenotype. When examined by transmission electron microscopy, the large platelets produced by a GP Ibβ^{Null} genotype revealed α-granules with increased size as compared with the α-granules from control mouse platelets. Data are presented linking the overexpression of a septin protein, SEPT5, to the presence of larger α-granules in the GP Ibβ^{Null} platelet. The *SEPT5* gene resides approximately 250 nucleotides 5′ to the *GP Ibβ* gene and has been associated with modulating exocytosis from neurons and platelets as part of a presynaptic protein complex. Fusion mRNA transcripts present in megakaryocytes can contain both the SEPT5 and GP Ibβ coding sequences as a result in an imperfect polyadenylation signal within the 3′ end of both the human and mouse *SEPT5* genes. We observed a 2- to 3-fold increase in SEPT5 protein levels in platelets from GP Ibβ^{Null} mice. These results implicate SEPT5 levels in the maintenance of normal α-granule size and may explain the variant granules associated with human GP Ibβ mutations and the Bernard-Soulier syndrome. (Blood. 2004;104:2339-2344)

Introduction

The Bernard-Soulier syndrome is a rare autosomal recessive disease resulting from mutations in any one of the 3 subunits comprising the platelet membrane receptor complex, glycoprotein (GP) Ib-IX.[1-3] The diagnostic features of the syndrome are a moderately reduced platelet count, visible giant platelets in peripheral blood smears, and an absent surface-expressed GP Ib-IX-V receptor. The presence or absence of a GP Ib-IX-V complex can be directly evaluated by flow cytometry and confirmed by the absence of ristocetin-induced platelet agglutination in platelet-rich plasma. A large number of mutations have been described producing the Bernard-Soulier phenotype, and what is readily apparent is the heterogeneous nature of the mutations within either of the 3 genes encoding the GP Ib-IX complex: *GP Ibα*, *GP Ibβ*, or *GP IX*.[3] However, mutations within the gene encoding the *GP V* subunit do not produce the Bernard-Soulier phenotype.[4,5]

A mouse model of the Bernard-Soulier syndrome has been described and was generated by the ablation of the GP Ibα subunit.[6] In this case, the most salient features of the human syndrome were all recapitulated by the mouse counterpart. Moreover, the phenotype was rescued by the expression of a transgene encoding human GP Ibα.[6] These results established proof that the absence of GP Ibα could directly produce the macrothrombocytopenic phenotype of the Bernard-Soulier syndrome. Detailed transmission electron microscopy of megakaryocytes and platelets from GP Ibα^{Null} animals revealed a reduction in cytoplasmic membrane content and suggested that normal megakaryocytopoiesis in the mouse is directly impacted by the presence of a GP Ib-IX complex.[7]

Here, we report the generation and characterization of a germ line knockout of the "other" subunit of GP Ib, GP Ibβ. Similar to their GP Ibα^{Null} counterparts, the animals display a severe bleeding phenotype and macrothrombocytopenia. However, transmission electron microscopy revealed the presence of increased granule size in platelets from GP Ibβ^{Null} animals. Indeed, one report on the molecular basis of the human Bernard-Soulier syndrome has linked abnormal platelet α-granules to a mutation in the human *GP Ibβ* gene.[8] This description remains the single report that documents platelet ultrastructure in a patient with a mutation in their *GP Ibβ* gene. Data will be presented and discussed linking the expression of platelet GP Ibβ to a nearby septin gene, *SEPT5*, implicated in exocytosis from platelets and neurons. The results suggest a role for the platelet septin, SEPT5, in the maintenance of granule morphology, and the implications for SEPT5 function are discussed.

Materials and methods

Isolation of the mouse GP Ibβ gene and construction of the targeting vector

A search of the high-throughput genomic sequence database using the mouse GP Ibβ cDNA sequence[9] identified a mouse clone (GenBank accession no. AC003067) containing 2 GP Ibβ exon sequences (Figure 1A).

From the Roon Research Center for Arteriosclerosis and Thrombosis, Division of Experimental Hemostasis and Thrombosi, Department of Molecular and Experimental Medicine, The Scripps Research Institute, La Jolla, CA; Unité Mixte de Recherche (UMR) 5533 Centre National de Recherche Scientifique (CNRS) Hôpital Cardiologique, Pessac, France; and the Department of Microbiology and Immunology, Dartmouth Medical School, Dartmouth-Hitchcock Medical Center, Lebanon, NH.

Submitted March 24, 2004; accepted May 18, 2004. Prepublished online as *Blood* First Edition Paper, June 22, 2004; DOI 10.1182/blood-2004-03-1127.

Supported by grants HL50545, HL42846, and HL69951 from the Heart, Lung, and Blood Institute of the National Institutes of Health (J.W.) and The Scripps Research Institute Skaggs Postdoctoral Fellowship Program (K.K.).

Reprints: Jerry Ware, Slot 505, University of Arkansas for Medical Sciences, 4301 W Markham St, Little Rock, AR 72205; e-mail: jware@uams.edu.

The publication costs of this article were defrayed in part by page charge payment. Therefore, and solely to indicate this fact, this article is hereby marked "advertisement" in accordance with 18 U.S.C. section 1734.

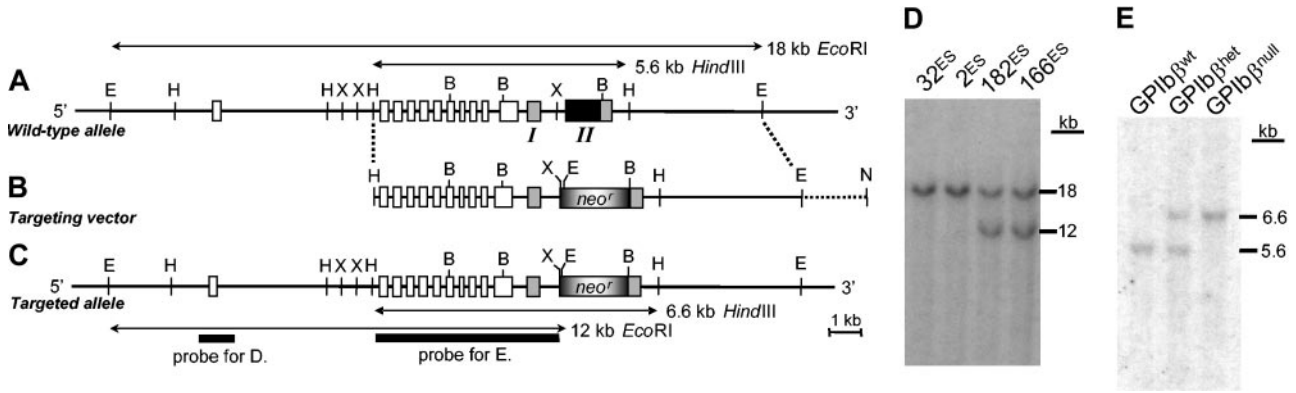

Figure 1. *GP Ibβ* gene structure and targeted disruption. (A) The mouse *GP Ibβ* gene is schematically presented as it spans a portion of GenBank accession no. AC008019. The *GP Ibβ* gene is adjacent to a second gene, *SEPT5*, whose exon arrangement is shown as open boxes. The *GP Ibβ* gene is composed of 2 exons (boxes I and II), with most of the coding sequence present in exon 2 (black box). E indicates *Eco*RI; H, *Hin*dIII; X, *Xho*I; and B, *Bam*HI. (B) The structure of a targeting vector to disrupt the *GP Ibβ* gene is shown directly under the corresponding genomic region depicted in panel A. The pBS/KS- vector is shown as a dashed line. N indicates *Not*I. (C) Successful homologous recombination in mouse embryonic stem (ES) cells results in the replacement of an 18-kb *Eco*RI restriction fragment with a 12-kb *Eco*RI fragment and the structure of a targeted allele is shown. The position of a radiolabeled probe used to identify clones with homologous recombination is shown. (D) Southern blot analysis of 2 clones (166^{ES} and 182^{ES}) with the altered *Eco*RI restriction fragment pattern and 2 clones (32^{ES} and 2^{ES}) with the 2 copies of a wild-type allele. (E) Germ line transmission of 166^{ES} cells was obtained producing GP $Ib\beta^{Het}$ mice. The breeding of GP $Ib\beta^{Het}$ mice produced the expected 3 genotypes and shown is a representative Southern blot of *Hin*dIII-restricted DNA revealing the wild-type GP Ibβ gene (5.6 kb) and the targeted allele (6.6 kb) present in each respective genotype.

The exon/intron arrangement for the mouse *GP Ibβ* gene is similar to the arrangement of the human *GP Ibβ* gene and contains the adjacent gene, *SEPT5* (previously designated as *CDCrel-1* and *PNUTL1*), immediately 5′ to the transcription start site of the *GP Ibβ* gene.[10-14]

To generate a targeting vector to ablate GP Ibβ expression, a 4.4-kb *Hin*dIII/*Xho*I restriction fragment spanning exon 1 was subcloned into pBS/KS- (Figure 1A). The new plasmid was further modified to add a neomycin-resistance (neo^r) cassette at the *Xho*I restriction site and generate a single plasmid containing the 5′ flanking arm and neo^r cassette (Figure 1B). A separate plasmid was generated to create the 3′ arm of the targeting vector corresponding to a 5.4-kb *Bam*HI/*Eco*RI restriction fragment spanning the 3′ end of exon 2 of GP Ibβ (Figure 1A). Then, utilizing a unique *Asc*I restriction site found 3′ to the neomycin cassette and a unique *Asc*I restriction site 5′ to the *Bam*HI restriction site in the 3′ arm, the 5′ arm, neo^r cassette, and 3′ arm were ligated together as depicted in Figure 1B. The targeting vector contains only the first 3 GP Ibβ codons of exon 1 and lacks all of the remaining GP Ibβ codons found in exon 2.

Generation of a platelet GP $Ib\beta^{Null}$ animal

The targeting vector was linearized with *Not*I and electroporated into DS2A embryonic stem (ES) cells. Transfected cells were selected for geneticin (G418) resistance and approximately 180 clones were expanded for analysis by Southern blotting. All probes were labeled by [^{32}P]dATP using a Prime-It II Random Primer Labeling kit (Stratagene, La Jolla, CA). Probe D was a 940–base pair (bp) *Dra*III/*Bsr*BI restriction fragment 5′ to the targeting vector (Figure 1C). Of the 180 different ES colonies, 5 revealed a Southern blot pattern consistent with the predicted change in a GP Ibβ allele (Figure 1C-D). Confirmation of the altered alleles was performed with Southern blot analysis of *Hin*dIII-digested genomic DNA probed with a labeled *Hin*dIII/*Xho*I restriction fragment (Figure 1C, probe E). Two transformed ES cell lines (182^{ES} and 166^{ES}) were chosen for injection into blastocysts and implantation into pseudopregnant females. Chimeras from both cell lines demonstrated germ line transmission and altered *GP Ibβ* alleles. Mice containing heterozygous GP Ibβ loci (GP $Ib\beta^{Het}$) were bred [GP $Ib\alpha^{Het}$ × GP $Ib\beta^{Het}$] and DNA analysis of the resultant offspring revealed all 3 expected GP Ibβ genotypes: wild-type (GP $Ib\beta^{WT}$), heterozygous (GP $Ib\beta^{Het}$), and homozygous-deficient (GP $Ib\beta^{Null}$) animals (Figure 1E).

Bleeding time assays

Mouse tail bleeding times were determined as previously described.[6] Briefly, a 1- to 3-mm portion of distal tail was removed, and the tail was immersed in isotonic saline (37°C). A complete cession of blood flow was defined as the bleeding time. When bleeding time exceeded 10 minutes, measurements were stopped by cauterization of the tails.

Flow cytometry

Whole blood was isolated from anesthesized mice from the retroorbital plexus.[15] Blood was collected in heparin-coated microhematocrit capillaries (Fisher Scientific, Pittsburgh, PA), and transferred to tubes with heparin at a final concentration of 30 U/mL (Sigma, St Louis, MO). Whole blood (2 μL) was mixed with 18 μL modified Tyrode buffer (5 mM HEPES [*N*-2-hydroxyethylpiperazine-*N*′-2-ethanesulfonic acid], pH 6.5; 137 mM NaCl, 2.7 mM KCl, 0.4 mM NaH_2PO_4, 2.8 mM dextrose) containing 1% bovine serum albumin. A quantity of 5 μL phycoerythrin (PE)–labeled rat antimouse GP Ibα monoclonal antibody (Xia.G5, M040-2; Emfret Analytics, Würzburg, Germany) or PE-labeled rat antimouse GPIIbIIIa (CD41/61) monoclonal antibody (Leo.D2, M020-2; Emfret Analytics) was then added, and the mixture was gently agitated and incubated for 15 minutes at room temperature. Phosphate-buffered saline (PBS; 400 μL) was added to each sample mixture immediately before the flow cytometry analysis. Measurements were obtained using a Becton Dickinson FACScan (San Jose, CA).

Immunoblotting

To make platelet lysates, murine blood was drawn from retroorbital bleeds as described in "Flow cytometry." Platelet-rich plasma (PRP) was obtained by centrifugation of whole blood at 500*g* (7 minutes, 4°C). Platelets were washed one time in a modified Tyrode buffer with 5 U/mL apyrase and 10 μM prostaglandin E1 and then centrifuged at 1500*g* (12 minutes). The platelet pellet was resuspended in 50 μL Tyrode buffer (pH 7.4) and lysed with an equal volume of 50 mM Tris (Tris(hydroxymethyl)aminomethane; pH 7.5) and 10% sodium dodecyl sulfate (SDS). Protein concentrations were determined using a Micro BCA kit from Pierce (Rockford, IL). Dithiothreitol (Sigma-Aldrich, St Louis, MO) was added as a final concentration of 10 mM to reduce protein samples before gel electrophoresis. Samples were boiled for 5 minutes and analyzed in a 4% to 20% gradient SDS–polyacrylamide gel electrophoresis (PAGE) gel. Following electrophoresis the proteins were transferred to nitrocellulose membranes (Invitrogen, Carlsbad, CA). Membranes were blocked with TBS-T (20 mM Tris [pH 7.5]; 150 mM NaCl, 0.05% Tween 20) containing 5% skim milk (30 minutes, room temperature).

The anti-SEPT5 monoclonal antibody, LJ-33, has been previously described.[16] The polyclonal anti-14-3-3ζ antibody was purchased from Santa Cruz Technologies (Santa Cruz, CA). Immunoreactive proteins were detected using a horseradish peroxidase (HRP)–conjugated rabbit anti-mouse immunoglobulin G (IgG) or HRP-conjugated goat antirabbit IgG

obtained from Zymed Laboratories (South San Francisco, CA). Primary antibodies were incubated with the membranes for 1 hour at room temperature. Afterward, the membranes were washed 3 times with TBS-T and the membranes were incubated with HRP-conjugated secondary antibody for 30 minutes at room temperature. Membranes were developed using an enhanced chemiluminescence detection system (Amersham-Pharmacia Biotech, Little Chalfont, United Kingdom).

Mouse brain lysates were prepared from dissected whole mouse brain. Briefly, the dissected brains were manually cut into small pieces, placed in a lysis buffer (150 mM NaCl, 1% Nonidet P-40, 0.5% sodium deoxycholate, 0.1% SDS, 10 μg/mL leupeptin, 10 mg/mL aprotinin, 1 mM Pefabloc, 50 mM Tris [pH 7.4]) and kept on ice prior to homogenization. Brains were then homogenized in a dounce homogenizer followed by 2 centrifugations to pellet insoluble material (3000*g*, 20 minutes, 4°C). Protein concentrations were determined using a Micro BCA kit (Pierce) and 20 μg of protein was analyzed by SDS-PAGE and immunoblotting.

Electron microscopy

Platelets were fixed in 1.25% glutaraldehyde (Fluka, Buchs, Switzerland) diluted in 0.1 M phosphate buffer (pH 7.2) for 1 hour at room temperature. Samples were washed and postfixed in 1% osmic acid containing 1.5% potassium ferrocyanide (Sigma) for 1 hour at 4°C. Following fixation the samples were dehydrated using graded alcohols and propylene oxide and then embedded in Epon (Taab Laboratories, Reading, United Kindom). Embedded samples were sectioned with an Ultracut E ultramicrotome (Reichert, Vienssa, Austria) and stained with uranyl acetate (Merck, Darmstadt, Germany) and lead citrate (Sigma).[17] The surface area of each platelet section was calculated for 41 randomly selected platelet sections using Metamorph software (Universal Imaging, Paris, France) as described.[7] The surface area of each α-granule within an individual platelet section was determined in a similar manner. The results (Table 2) are expressed as mean values plus or minus standard deviation (SD). Statistical analysis was performed by means of the Student *t* test.

Results

The mouse GP Ibβ cDNA sequence has been previously reported along with a BAC clone containing the mouse *GP Ibβ* gene.[9,13] Figure 1 displays a diagrammatic representation of the 2 exons encoding platelet GP Ibβ and also displays the close proximity of another gene, termed *SEPT5* (previously designated *CDCrel-1*), whose 3′ end is approximately 250 nucleotides 5′ to exon 1 of the *GP Ibβ* gene.[10,12,14] The close proximity of the 2 genes results in a transcriptionally complex locus owing to the presence of an aberrant polyadenylation signal sequence within the *SEPT5* gene.[10] As a result of imperfect polyadenylation, a number of different transcripts have been described containing SEPT5, GP Ibβ, and SEPT5/GP Ibβ mRNA sequences.[10] Both SEPT5 and GP Ibβ transcripts and proteins have been identified in platelets, suggesting both genes may share regulatory elements that support megakaryocytic expression.[11,16]

To generate a targeted replacement of the mouse *GP Ibβ* gene, a targeting vector was generated in which all of the codons in GP Ibβ exon 2 were replaced with a neo^r cassette (Figure 1B and "Materials and methods"). Transfection of the targeting vector into mouse embryonic stem (ES) cells and selection for neomycin resistance produced 180 antibiotic-resistant ES cell lines. A Southern blot analysis of all 180 clones identified 5 clones with the predicted change in a single GP Ibβ allele (Figure 1C-D). Of the 5 clones, 2 (166^{ES} and 182^{ES}) were chosen to generate chimeric animals and chimeric males from both cell lines produced germ line transmission of the altered ES cell genotype. Heterozygous animals (GP $Ib\beta^{Het}$) were chosen for the generation of a GP Ibβ knockout colony. The breeding of heterozygous animals produced offspring with the expected genotypes: wild-type (GP $Ib\beta^{WT}$), heterozygous (GP $Ib\beta^{Het}$), and knockout (GP $Ib\beta^{Null}$) (Figure 1E). No problems with breeding or viability have been observed in the GP $Ib\beta^{Null}$ colony just as previously described for GP $Ib\alpha^{Null}$ animals.[6]

The role of GP Ibβ in the efficient surface expression of a GP Ib-IX complex has been established in transfection studies using heterologous cells.[18-20] The expression of a mouse GP Ib-IX complex on the surface of platelets from mice with altered GP Ibβ alleles was analyzed by flow cytometry. As shown in Figure 2A, GP $Ib\beta^{Null}$ platelets have no detectable GP Ib-IX complex assayed with a PE-labeled rat antimouse GP Ibα antibody. Platelets produced from animals with GP $Ib\beta^{Het}$ alleles express GP Ib-IX complex but are clearly different from their GP $Ib\beta^{WT}$ littermates, presumably owing to a lower platelet count and increased platelet size (Figure 2C). The expression of the murine integrin complex, αIIb/β3, was also examined in the same animals. In the absence of a GP Ib-IX complex, increased fluorescence for αIIb/β3 was observed for both GP $Ib\beta^{Null}$ and GP $Ib\alpha^{Null}$ platelets. A hallmark feature of Bernard-Soulier platelets is their large size, and this was apparent for GP $Ib\beta^{Null}$ platelets by monitoring their forward-light scatter profile (Figure 2C). GP $Ib\beta^{Het}$ platelets displayed an intermediate size similar to that reported for GP $Ib\alpha^{Het}$ platelets.[6]

Having established the presence of giant platelets in GP $Ib\beta^{Null}$ animals, we examined hematologic parameters for littermates produced from GP $Ib\beta^{Het}$ × GP $Ib\beta^{Het}$ crosses. As summarized in Table 1, erythrocyte count, hemoglobin levels, microhematocrit, and white blood cell count were all indistinguishable in the blood of GP $Ib\beta^{WT}$, GP $Ib\beta^{Het}$, and GP $Ib\beta^{Null}$ genotypes. However, platelet counts were influenced by the presence or absence of GP Ibβ alleles. Platelet counts in GP $Ib\beta^{Null}$ animals were approximately 25% of the levels present in wild-type littermate controls.

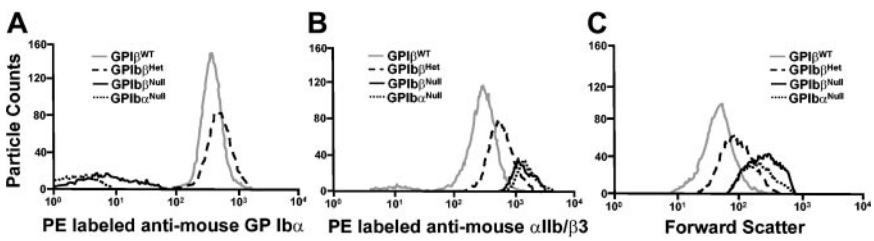

Figure 2. Flow cytometric analysis. (A) A flow cytometric analysis of whole blood was performed after labeling with a PE-tagged rat antimouse GP Ibα monoclonal antibody. Surface expression of a GP Ib-IX complex requires concomitant expression of GP Ibα, GP Ibβ, and GP IX. As shown, neither blood from GP $Ib\beta^{Null}$ nor GP $Ib\alpha^{Null}$ animals contains a reactive anti-GP Ibα signal. (B) Mouse integrin, αIIb/β3 levels are shown in mice deficient in a GP Ib-IX complex. A PE-tagged rat antimouse αIIb/β3 monoclonal antibody was mixed with whole blood and samples were analyzed by flow cytometry. An increase in αIIb/β3 levels in heterozygotes and homozygotes probably reflects an increase in platelet volume per platelet. (C) Forward-scatter profile of platelets from the designated mice are presented. Both GP $Ib\alpha^{Null}$ and GP $Ib\beta^{Null}$ platelets have a similar increased platelet size in their population. GP $Ib\beta^{Het}$ platelet size presents as an intermediate phenotype between wild-type and knockout platelets.

Table 1. Blood counts

	GP Ibβ^{WT} n = 5	GP Ibβ^{het} n = 6	GP Ibβ^{null} n = 6
RBC count, × 10^{12}/L	8.09 (0.55)	7.58 (0.42)	8.48 (1.26)
Hg, g/L	143 (9)	135 (6)	153 (20)
PCV, % microhematocrit	39.9 (2.3)	38.0 (1.5)	43.3 (5.9)
WBC count, × 10^9/L	6.62 (2.56)	8.70 (1.39)	8.40 (1.62)*
Platelet count, × 10^9/L	955 (76)	805 (89)†	241 (47)‡

Values are presented as the mean, with the standard deviation in parentheses. RBC indicates red blood cell; Hg, hemoglobin; PCV, packed cell volume; and WBC, white blood cell.

*n = 5.

†P = .014 using Student t test for a comparison with GP Ibβ^{WT}.

‡$P = 8.60 \times 10^{-7}$ using Student t test for a comparison with GP Ibβ^{WT}.

GP Ibβ^{Het} animals had an intermediate platelet count similar to that reported from GP Ibα^{Null} animals.[6] The decrease in circulating platelet counts was significant for both GP Ibβ^{Het} and GP Ibβ^{Null} animals (Table 1).

As a final assay to verify that the GP Ibβ^{Null} phenotype produces a murine equivalent of the Bernard-Soulier syndrome, tail bleeding times were determined for each of the 3 genotypes (Figure 3). Just as reported for GP Ibα^{Null} animals, GP Ibβ^{Null} animals display a severe bleeding phenotype as expected for the congenital absence of a major platelet adhesion receptor.

The ultrastructure of GP Ibα^{Null} mouse platelets has been previously described and with the exception of the larger platelet size and abnormal membrane distribution, no other distinguishing characteristics were noted.[7] However, transmission electron microscopy of GP Ibβ^{Null} platelets revealed an unexpected finding; namely, the α-granules appeared to be larger than their counterparts in normal mouse platelets (Figure 4). To quantify this change, the area occupied by α-granules in 41 random platelet sections was measured. As summarized in Table 2, the mean platelet area of 41 platelet sections was larger in GP Ibβ^{Null} platelets (2.95 μm^2 vs 1.69 μm^2), consistent with the presence of larger platelets in the population. The total number of granules in the 41 sections was larger in the GP Ibβ^{Null} samples (215 vs 150) but when normalized for the platelet area, the number of granules per μm^2 was less in GP Ibβ^{Null} samples (1.78 vs 2.17). However, the average surface area occupied by a single α-granule in the GP Ibβ^{Null} platelet was larger than the average surface area of an α-granule from a control platelet sample (0.090 μm^2 vs 0.074 μm^2; P = .0006). The larger α-granules did not reflect more α-granule content, as α-granules occupied 16% of the total area in both knockout and control samples (Table 2). Thus, GP Ibβ^{Null} platelets have fewer α-granules per μm^2 of section, but those present are slightly larger. The total cytoplasmic area occupied by α-granules is the same for a GP Ibβ^{WT} or GP Ibβ^{Null} platelet.

Given our prior studies that documented the close proximity of the *GP Ibβ* gene to a septin gene, *SEPT5*, along with a growing awareness of SEPT5 as part of a presynaptic complex in neurons and platelet vesicles, we hypothesized that ablation of the *GP Ibβ* gene has altered SEPT5 levels. Shown in Figure 5A is a Western blot analysis of SEPT5 levels in resting mouse platelets. GP Ibβ^{Null} platelets displayed an approximate 2- to 3-fold increase in SEPT5 protein levels. GP Ibβ^{Het} platelets had an intermediate level of SEPT5 protein, whereas SEPT5 levels in GP Ibα^{Null} platelets were similar to wild-type controls. Since SEPT5 is also expressed to high levels in brain, we examined SEPT5 levels in brain lysates. Here the levels of SEPT5 were indistinguishable among GP Ibβ^{WT}, GP Ibβ^{Null}, and GP Ibα^{Null} samples. Thus, the increased levels of SEPT5 protein is unique to the megakaryocytic lineage and does not occur in brain tissue.

Discussion

The etiology of the Bernard-Soulier syndrome is well established with numerous mutations found in the *GP Ibα*, *GP Ibβ*, and *GP IX* genes.[1,3] In all cases, the diagnosis usually starts with recognition of the hallmark features of the phenotype, macrothrombocytopenia, a lack of ristocetin-induced platelet aggregation, and undetectable GP Ib-IX-V complex by flow cytometry. At the molecular level, the heterogeneity of the syndrome becomes apparent as a full range of genetic lesions, missense mutations, nonsense mutations, and gene deletions have each been described in individual pedigrees. The unifying feature of all of the mutations is the ability of the mutation to disrupt the assembly and function of a surface-expressed GP Ib-IX-V complex. How individual mutations affect complex assembly or surface expression can be variable. Indeed, in many instances an individual who has been identified as a carrier of the Bernard-Soulier phenotype (heterozygous) may have partial macrothrombocytopenia,[21-23] yet in other cases the platelets from carriers are indistinguishable from normal platelets.[24,25] Relative to the heterogenous nature of mutations in the GP Ibβ gene was the description of a Bernard-Soulier variant with the appearance of abnormal granules in the cytoplasm, a unique finding never before associated with a Bernard-Soulier phenotype.[8] A presumed second mutation, unrelated to the GP Ib-IX-V complex, or some unknown link between the GP Ib-IX-V complex and platelet vesicle formation was suggested as the basis for this secondary finding.[8] Nevertheless, recognizing the heterogeneity that gives rise to the Bernard-Soulier syndrome is a first step at understanding all aspects of the receptor and how it participates in hemostasis, thrombosis, and platelet formation.

As a continuing effort on the development of mouse models of hemostasis and thrombosis we targeted the mouse GP Ibβ gene. Our results demonstrated that the most salient features of the Bernard-Soulier syndrome were present in the GPIbβ^{Null} murine model. The thrombocytopenia (Table 1), lack of a surface-expressed GP Ib-IX-V complex (Figure 2A), large platelets (Figure 2C), and severe bleeding (Figure 3) established the generation of the model and validated its phenotypic similarity to the mouse

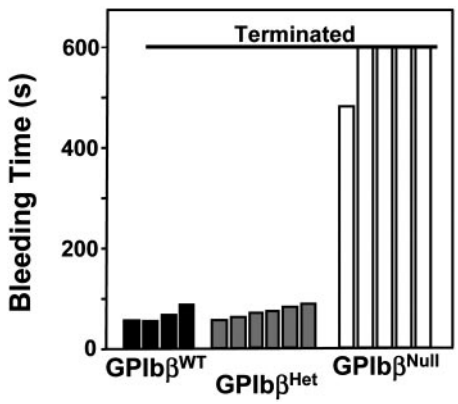

Figure 3. Tail bleeding time assays. Offspring produced from GP Ibβ^{Het} × GP Ibβ^{Het} crosses were subjected to tail bleeding time assays prior to their genotyping. Results are shown for 5-week-old animals and the cessation of bleeding time was recorded. Four animals, later genotyped as GP Ibβ^{Null}, failed to stop by bleeding by 10 minutes, at which point the tail was cauterized. Shown are the data obtained from individual animals.

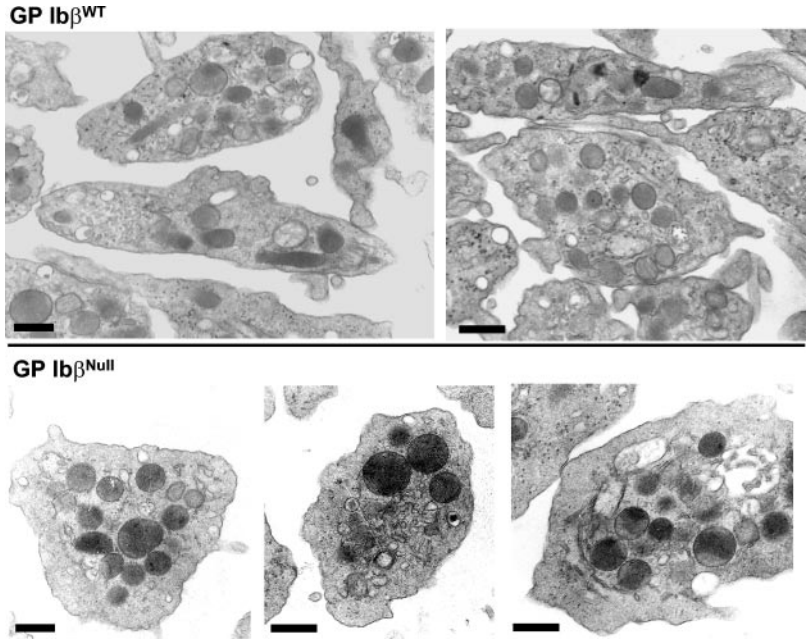

Figure 4. Transmission electron microscopy of purified platelets. Platelet-rich plasma was prepared and a platelet pellet was fixed with glutaraldehyde. After osmium staining, platelet samples were viewed by electron microscopy. Shown are representative sections from GP Ibβ^{WT} and GP Ibβ^{Null} platelets. A black bar in each panel represents 500 nm. Platelet areas and α-granule areas were quantified from 41 randomly selected sections and the results are presented in Table 2. Images were obtained using a Jeol JEM-1010 transmission electron microscope (Jeol, Croissy-sur-seine, France) at 80 kV. Quantitation of surface areas was calculated using Metamorph software (Universal Imaging, Paris, France).

Bernard-Soulier model generated by ablation of the GP Ibα gene.[6] By all of the previously mentioned criteria, the phenotype of a GP Ibα^{Null} and GP Ibβ^{Null} animal were indistinguishable. However, when we examined transmission electron microscopic images of the GP Ibβ^{Null} platelets, a noticeable increase in α-granule size was apparent (Figure 4). A more objective analysis of the α-granule size was obtained by quantifying platelet size and determining the cytoplasmic area of each platelet occupied by α-granules. Here, the results confirmed the ablation of the GP Ibβ gene had increased α-granule size while the area of the cytoplasm occupied by α-granules had not changed (Table 2).

A similar increase in α-granule size was not observed with GP Ibα^{Null} platelets,[6,7] so we considered the possibility that the molecular basis of the increased granule size was not directly linked to the GP Ib-IX-V complex. Instead, we considered the possibility that by deleting a large portion of the GP Ibβ transcript, we effected the expression of a septin gene, *SEPT5*, located immediately 5′ to the platelet *GP Ibβ* gene (Figure 1). We originally described SEPT5 as part of a transcriptionally complex locus composed of the *CDCrel-1* (later renamed *SEPT5*[14]) and *GP Ibβ* genes.[10] A potential role for SEPT5 in α-granule biology is not completely unexpected. Both in platelets and in neurons SEPT5 is part of a presynaptic protein complex and inhibits the soluble NSF attachment protein receptor (SNARE)–protein syntaxin, thereby negatively modulating neurotransmitter release and platelet release.[16,26,27] Increased levels of SEPT5 in GP Ibβ^{Null} platelets suggest that SEPT5 influences platelet granule morphology (Figure 5). Increased levels of SEPT5 were not observed in brain lysates, suggesting the alteration of SEPT5 levels is specific to megakaryocytic expressed transcripts from the *SEPT5*/*GP Ibβ* locus. We have also examined platelets that are devoid of SEPT5.[16] Here, the platelets release stored components in the presence of subthreshold levels of agonist but no noticeable differences are seen in α-granule morphology (J.W. and P.N., unpublished observation, March 1999). Thus, the increased level of SEPT5 in the GP Ibβ^{Null} platelet may not have a role in the biogenesis of platelet granules but may be causing a premature vesicle fusion. Such a possibility is

Table 2. Analysis of transmission electron microscope platelet sections

	GP Ibβ^{WT}	GP Iβ^{Null}
Platelet section area, μm^2, mean (SD)	1.690 (0.941)	2.947 (0.724)
Platelet section area, no. patients	41	41
No. of ∞-granules in 41 sections	150	215
Surface of granules, μm^2, mean (SD)	0.0743 (0.0356)*	0.0900 (0.0319)*
Surface of granules, no. patients	150	215
% of platelet area with ∞-granules (total granule area/total platelet area)	16	16
No. of granules per μm^2	2.17	1.78

*P = .0006 using the Student t test.

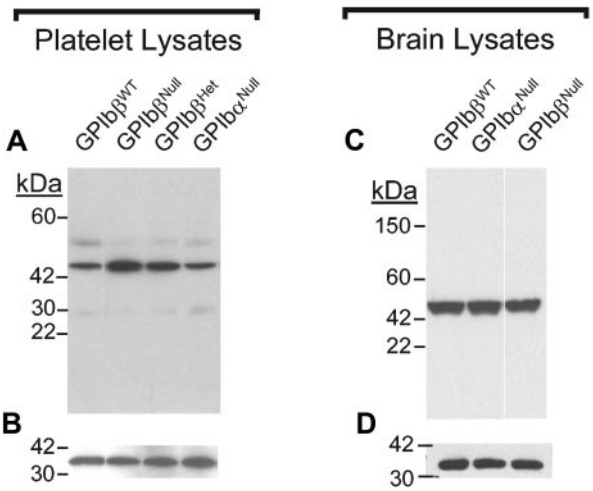

Figure 5. SEPT5 levels in platelet and brain lysates. (A) Protein concentrations in mouse platelet lysates samples were determined and similar protein amounts were loaded into a reducing 4% to 20% SDS-PAGE. After electrophoresis, the proteins were transferred to nitrocellulose and immunoblotted with an anti-SEPT5 monoclonal antibody (LJ-33). As previously shown, the predominant SEPT5 signal present in platelet lysates is approximately 45 kDa. Quantitation revealed a 2- to 3-fold increase in SEPT5 levels in platelets from GP Ibβ^{Null} animals. (B) The same membrane was subsequently reacted with an anti-14-3-3ζ polyclonal antibody to document the approximate protein load for each lane using 14-3-3ζ (32 kDa) as an internal standard. (C) Equal quantities of brain lysates protein were analyzed by SDS-PAGE and immunoblotting for the septin protein, SEPT5. (D) The filter shown in panel C was reprobed for 14-3-3ζ protein and is shown for comparison.

suggested by the similar cytoplasmic areas occupied by α-granules in either a GP Ibβ^{Null} or GP Ibβ^{WT} platelet (Table 2).

How would the gene deletion created to produce a GP Ibβ^{Null} locus alter levels of the SEPT5 protein? We previously described the presence of a megakaryocytic transcript containing a fusion of SEPT5 and GP Ibβ mRNA sequences.[10] In the current work, our targeting strategy generated a locus where a large part of *GP Ibβ* exon 2 has been replaced by the neo^r cassette (Figure 1C). Thus, a potential scenario has developed where there is increased stability in a transcript encoding SEPT5 in the SEPT5/GP Ibβ fusion transcript. As such, the fusion transcript containing SEPT5 and GP Ibβ sequences becomes relevant to the megakaryocytic expression of SEPT5. It would also suggest that a similar fusion transcript is not relevant to neuron-expressed SEPT5, since SEPT5 levels were unchanged in brain tissue.

The close proximity of the *GP Ibβ* and *SEPT5* genes certainly supports the possibility that the expression of one gene might influence the expression level of the other. Are larger α-granules to be an expected finding for GP Ibβ mutations associated with the Bernard-Soulier phenotype? We believe this is unlikely and would depend on the specific mutation in the *GP Ibβ* gene. Several of the *GP Ibβ* gene mutations that have been described are missense mutations.[23,28-30] In general, these mutations might be expected to have a minimal effect on transcript stability. However, in the case of Watanabe et al,[8] who observed abnormal vesicles, the mutation is a 13-bp deletion within the signal peptide coding region of the *GP Ibβ* gene. In this case, the transcript stability may have changed and could represent the etiology of the variant granules.

The recognition of mammalian septins as critical regulators of cytoplasmic events is growing.[31,32] Our results examining the phenotype of GP Ibβ-deficient platelets provide some unexpected findings relevant to septin biology and identify some future experiments to dissect septin relevance in platelet biology. An unexpected phenotype in the Bernard-Soulier mouse has contributed both on the role of GP Ib-IX and of septins for normal platelet structure and function. Thus, new directions for future studies are provided by the GP Ibβ^{Null} animal.

Acknowledgments

The authors acknowledge the Sam and Rose Stein Charitable Trust for the establishment of the DNA Core Facility within the Department of Molecular and Experimental Medicine at The Scripps Research Institute. The administrative support of Ms Pamela Fagan is greatly appreciated.

References

1. Lopez JA, Andrews RK, Afshar-Kharghan V, Berndt MC. Bernard-Soulier syndrome. Blood. 1998;91:4397-4418.
2. Berndt MC, Shen Y, Dopheide SM, Gardiner EE, Andrews RK. The vascular biology of the glycoprotein Ib-IX-V complex. Thromb Haemost. 2001; 86:178-188.
3. Kunishima S, Kamiya T, Saito H. Genetic abnormalities of Bernard-Soulier syndrome. Int J Hematol. 2002;76:319-327.
4. Ramakrishnan V, Reeves PS, DeGuzman F, et al. Increased thrombin responsiveness in platelets from mice lacking glycoprotein V. Proc Natl Acad Sci U S A. 1999;96:13336-13341.
5. Kahn ML, Diacovo TG, Bainton DF, Lanza F, Coughlin SR. Glycoprotein V-deficient platelets do not exhibit a Bernard-Soulier phenotype and retain normal thrombin responsiveness. Blood. 1999;94:4112-4121.
6. Ware J, Russell S, Ruggeri ZM. Generation and rescue of a murine model of platelet dysfunction: the Bernard-Soulier syndrome. Proc Natl Acad Sci U S A. 2000;97:2803-2808.
7. Poujol C, Ware J, Nieswandt B, Nurden AT, Nurden P. Absence of GP Ibα is responsible for the aberrant membrane development during megakaryocyte differentiation: an ultrastructural study. Exp Hematol. 2002;30:352-360.
8. Watanabe R, Ishibashi T, Saitoh Y, et al. Bernard-Soulier syndrome with a homozygous 13 base pair deletion in the signal peptide-coding region of the platelet glycoprotein Ibβ gene. Blood Coag Fib. 2003;14:1-8.
9. Kitaguchi T, Murata M, Anbo H, Moriki T, Ikeda Y. Characterization of the gene encoding mouse platelet glycoprotein Ibβ. Thromb Res. 1997;87: 235-244.
10. Zieger B, Hashimoto Y, Ware J. Alternative expression of platelet glycoprotein Ibβ mRNA from an adjacent 5′ gene with an imperfect polyadenylation signal sequence. J Clin Invest. 1997;99: 520-525.
11. Yagi M, Edelhoff S, Disteche CM, Roth GJ. Structural characterization and chromosomal location of the gene encoding human platelet glycoprotein Ibβ. J Biol Chem. 1994;269:17424-17427.
12. Yagi M, Zieger B, Roth GJ, Ware J. Structure and expression of the human septin gene HCD-CREL-1. Gene. 1998;212:229-236.
13. Peng X-R, Jia Z, Ware J, Trimble WS. The septin CDCrel-1 is dispensable for normal development and neurotransmitter release. Mol Cell Biol. 2002; 22:378-387.
14. Macara IG, Baldarelli R, Field CM, et al. Mammalian septins nomenclature. Mol Biol Cell. 2002;13: 4111-4113.
15. Hoff J. Methods of blood collection in the mouse. Lab Animal. 2004;29:47-53.
16. Dent J, Kato K, Peng X-R, et al. A prototypic platelet septin and its participation in platelet secretion. Proc Natl Acad Sci U S A. 2002;99:3064-3069.
17. Poujol C, Tronik-Le Roux D, Tropel P, et al. Ultrastructural analysis of bone marrow hematopoiesis in mice transgenic for the thymidine kinase gene driven by the α_{IIb} promoter. Blood. 1998;92:2012-2023.
18. Lopez JA, Leung B, Reynolds CC, Li CQ, Fox JEB. Efficient plasma membrane expression of a functional platelet glycoprotein Ib-IX complex requires the presence of its three subunits. J Biol Chem. 1992;267:12851-12859.
19. Lopez JA, Weisman S, Sanan DA, et al. Glycoprotein (GP) Ibβ is the critical subunit linking GP Ibα and GP IX in the GP Ib-IX complex. J Biol Chem. 1994;269:23716-23721.
20. Strassel C, Pasquet JM, Alessi MC, et al. A novel missense mutation shows that GPIbbeta has a dual role in controlling the processing and stability of the platelet GPIb-IX adhesion receptor. Biochemistry. 2003;42:4452-4462.
21. De Marco L, Mazzucato M, Fabris F, et al. Variant Bernard-Soulier syndrome type Bolzano: a congenital bleeding disorder due to a structural and functional abnormality of the platelet glycoprotein Ib-IX complex. J Clin Invest. 1990;86:25-31.
22. Savoia A, Balduini CL, Savino M, et al. Autosomal dominant macrothrombocytopenia in Italy is most frequently a type of heterozygous Bernard-Soulier syndrome. Blood. 2001;97:1330-1335.
23. Kurokawa Y, Ishida F, Kamijo T, et al. A missense mutation (tyr88 to cys) in the platelet membrane glycoprotein Ibbeta gene affects GPIb/IX complex expression: Bernard-Soulier syndrome in the homozygous form and giant platelets in the heterozygous form. Thromb Haemost. 2001;86: 1249-1256.
24. Hillmann A, Nurden A, Nurden P, et al. A novel hemizygous Bernard-Soulier Syndrome (BSS) mutation in the amino terminal domain of glycoprotein (GP)Ibβ-platelet characterization and transfection studies. Thromb Haemost. 2002;88: 1026-1032.
25. Nurden AT, Combrie R, Claeyssens S, Nurden P. Heterozygotes in the bernard-soulier syndrome do not necessarily have giant platelets or thrombocytopenia. Br J Haematol. 2003;120:716-717.
26. Beites CL, Xie H, Bowser R, Trimble WS. The septin CDCrel-1 binds syntaxin and inhibits exocytosis. Nature Neurosci. 1999;2:434-439.
27. Beites C, Peng X-R, Trimble WS. Expression and analysis of properties of septin CDCrel-1 in exocytosis. Methods Enzymol. 2001;329:499-510.
28. Kunishima S, Lopez JA, Kobayashi S, et al. Missense mutations of the glycoprotein (GP) Ib beta gene impairing the GPIb alpha/beta disulfide linkage in a family with giant platelet disorder. Blood. 1997;89:2404-2412.
29. Kunishima S, Tomiyama Y, Honda S, et al. Homozygous Pro74→Arg mutation in the platelet glycoprotein Ibbeta gene associated with Bernard-Soulier syndrome. Thromb Haemost. 2000; 84:112-117.
30. Kunishima S, Naoe T, Kamiya T, Saito H. Novel heterozygous missense mutation in the platelet glycoprotein Ib beta gene associated with isolated giant platelet disorder. Am J Hematol. 2001; 68:249-255.
31. Kartmann B, Roth D. Novel roles for mammalian septins: from vesicle trafficking to oncogenesis. J Cell Sci. 2001;114:839-844.
32. Kinoshita M. Assembly of mammalian septins. J Biochem (Tokyo). 2003;134:491-496.